Title: The phenomenal properties of color experience have exact analogs in the mathematical properties of qubit mixtures

Author: Tal Hendel, hendeltal@gmail.com

Date: 25.3.2023

Status: Submitted

Abstract

Our color experience contains six elementary color sensations: white, black, red, yellow, green, and blue. All colors are perceived as some combination of two, three, or four of these elementary colors. The six elementary colors fall into two phenomenally distinct groups: two achromatic elementary colors (white and black) vs. four elementary hues. Newton noticed that the gamut of all hues can be arranged in a closed continuum known as the hue circle. Hering pointed out that there are no combinations of red and green or yellow and blue along this circle. To explain this, he suggested that our chromatic sensations arise from two pairs of opponent processes: a red–green pair and a yellow–blue pair. A white–black pair of achromatic opponent processes was suggested to account for the sensation of lightness. The achromatic opponent processes are noticeably different from their chromatic counterparts in that the elementary colors in this pair, white and black, clearly do combine to yield a phenomenal mixture, i.e., gray. A fourth dimension of color is its brightness, i.e., its perceived intensity. Although phenomenally distinct, there is an ill-understood relationship between lightness and brightness. What brings about these and other conspicuous properties of color

experience? Here I show that the phenomenal properties of color experience have remarkable analogs in the mathematical properties of qubit states reconstructed through quantum state tomography. I therefore hypothesize that color experience may be the phenomenal dual aspect of a qubit ensemble undergoing quantum state tomography somewhere in the brain.

1. Introduction

Our color experience contains six elementary color sensations: white, black, red, yellow, green, and blue. What makes these colors elementary is that they 'have no characteristic resemblance to each other, while all other color percepts remind us of two, three, or four of these six' (Hård et al., 1996, p. 184). It is immediately evident that the six elementary colors fall into two phenomenally distinct groups: a pair of achromatic elementary colors (white and black) vs. four elementary hues. Each of the elementary hues has a focal example that is referred to as *unique* since it is perceived as unmixed. For example, unique red is the variant of red that exhibits no hint of yellow or of blue. As was first observed by Newton (Kuehni, 2003, chapter 2), the gamut of all hues can be arranged in a *closed* continuum: starting (arbitrarily) with unique red, we move through shades of yellowish reds and reddish yellows to unique yellow; from unique yellow we continue through shades of greenish yellows and yellowish greens to unique green; from unique green we continue through shades of bluish greens and greenish blues to unique blue; and from unique blue, through shades of reddish blues and bluish reds, we return to unique red, where we started. This closed continuum is ordinarily portrayed as a circle. Hering, in the latter part of the 19th century, pointed out that there are no combinations of red and green or combinations of yellow and blue along the hue circle (i.e., there are no reddish greens, greenish reds, yellowish blues, or bluish yellows on this circle) (*ibid*.). To explain this observation, he suggested that our chromatic sensations arise from two mechanisms of *opponent elementary processes*: a red–green mechanism and a yellow–blue mechanism (Hurvich & Jameson, 1957). To account for the achromatic colors, Hering further suggested that white and black processes operate as a third opponent pair of elementary processes (*ibid*.). The gamut of all outputs of the white–black mechanism gives rise to a continuum of achromatic colors that runs from black through grays to white. The phenomenal attribute that varies along this continuum is known as lightness. Notice, then, that the achromatic pair of opponent processes is very different from its chromatic counterparts in that white and black clearly do combine to yield a phenomenal mixture, i.e., gray.

According to Hering, then, there exist three color mechanisms (or channels). Let us denote the red–green, yellow–blue, and white–black mechanisms by $(R-G)$, $(Y-B)$, and $(W-S)$, respectively. I will assume that the output of each mechanism is bounded by 1 from above and by -1 from below. That is, $-1 \leq (R-G) \leq 1$, and so on for the other two mechanisms. When the output of an opponent-processes mechanism is 0, the evoked sensation is that of middle gray, i.e., gray that is perceptually midway between black and white. When the output of an opponent-processes mechanism is at an extremum (i.e., -1 or 1), the evoked sensation is *pure*, namely, it does not contain any grayness in it. For example, when $(W-S)=1$, the evoked sensation is of pure white, i.e., white that exhibits no hint of grayness (and no hint of hue, of course). As the output of each mechanism moves from 1 to 0, the purity of the evoked sensation diminishes from 1 to 0 (concurrently, of course, the proportion of grayness in the evoked sensation increases from 0 to 1). Then, as the output of the mechanism moves from 0 to -1, the purity of the color sensation gradually increases from 0 to 1. Notably, the hue sensations evoked by each of the two chromatic mechanisms are the unique variants of their respective hues. That is, the red–green mechanism gives rise to unique red and unique green and the yellow–blue mechanism gives rise to unique yellow and unique blue. As mentioned earlier, these sensations will not be pure unless the mechanism's output is at an extremum. For example, when $(R-G)=1$, the evoked sensation is of pure unique red; when $(R-G)=-1$, the evoked sensation is of pure unique green.

Hering's theory of color experience can be visualized in the three-dimensional space shown in Fig. 1.

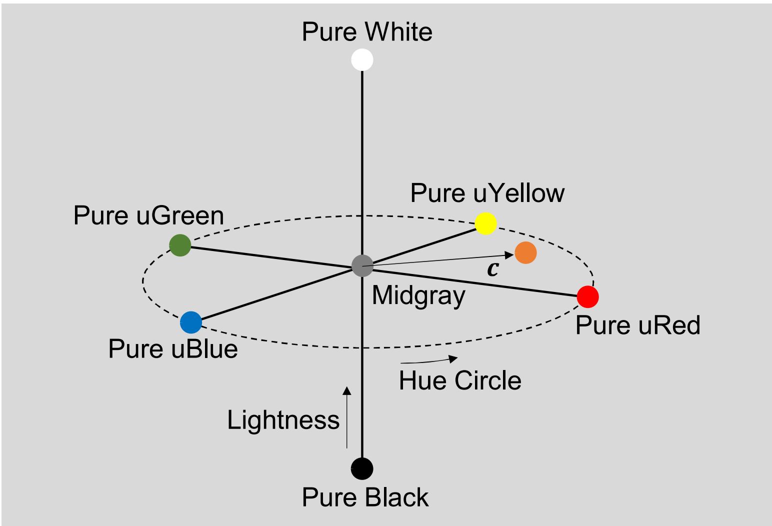

Figure 1. A scheme of phenomenal color space according to Hering. Any color percept can be represented as a vector in this three-dimensional space. One example, $\boldsymbol{c}$, is shown in the figure. Hering's three pairs of opponent elementary color sensations are arranged as three antipodal pairs: pure white vs. pure black, pure unique red vs. pure unique green, pure unique yellow vs. pure unique blue. The continuous curve between the four unique hues constitutes the hue circle.

The scheme of Fig. 1 is similar in nature to other color spaces that follow 'Heringian' principles (for a historical review of such color spaces, see Kuehni, 2003, chapter 2). The most famous and most thoroughly worked out of these color spaces is the Swedish Natural Color System (NCS) (Hård et al., 1996).[1] If we assign the output of the red–green mechanism to the x-axis in Fig. 1, the output of the yellow–blue mechanism to the y-axis, and the output of the white–black mechanism to the z-axis, any color percept can then be represented as a vector in Cartesian coordinates in the following manner:

$$\boldsymbol{c} = (R - G)\hat{\boldsymbol{\imath}} + (Y - B)\hat{\boldsymbol{\jmath}} + (W - S)\hat{\boldsymbol{k}}, \tag{1}$$

where $\hat{\boldsymbol{\imath}}$, $\hat{\boldsymbol{\jmath}}$, $\hat{\boldsymbol{k}}$ are the standard basis vectors of $\mathbb{R}^3$. One example of such a vector is shown in Fig. 1.

When two color stimuli are additively mixed, the resulting color percept is a weighted mixture of the two original percepts, where the weights are determined by the relative amounts of the addends in the mixture. This is the well-known 'center of gravity principle' of color addition (Boynton, 1979, chapter 5). Using the vector representation of color percepts in Eq. 1, this principle can easily be formalized: if we additively mix N_1

[1] In contrast to the scheme of color space of Fig. 1, the NCS does not use Cartesian coordinates to represent color vectors.

units of a color vector $\boldsymbol{c}_1$ with N_2 units of a color vector $\boldsymbol{c}_2$, the resultant color vector is given by

$$\boldsymbol{c} = \frac{N_1}{N_1 + N_2}\boldsymbol{c}_1 + \frac{N_2}{N_1 + N_2}\boldsymbol{c}_2. \tag{2}$$

Of course, Eq. 2 can be generalized to any number of color addends.[2] Notably, at high intensities (i.e., when N_1 and N_2 are large), the linearity of this equation breaks down (see review of evidence in Shevell, 2003) and it only gives an approximation of the results of color addition.

Note that if Hering's three color mechanisms are assumed to be independent, then a consequence of Eq. 2 is that phenomenal color space should have the shape of a double-square pyramid. In such a space, the hue circle becomes a *hue square*. To see why, suppose, for example, that for some light stimulus we have $(R - G) = 1$, which gives rise to pure unique red. Further suppose that the same light stimulus also leads to $(Y - B) = 1$, which gives rise to pure unique yellow. According to Eq. 2, the resultant evoked sensation will be of an orange color located in the middle of the line connecting

[2] Equation 2 is the basis for color matching experiments: any color $\boldsymbol{c}$ can be matched by a correctly weighted mixture of three (or more) different colors $\boldsymbol{c}_1$, $\boldsymbol{c}_2$, and $\boldsymbol{c}_3$ (Boynton, 1979, chapter 5). It is often stated that although equations like Eq. 2 'express the conditions for a color match, they do not tell us anything directly about what the matching colors look like' (*ibid*., p. 136). Here, however, following Hering, the components of color vectors are specified by the *phenomenal* attributes red–green, yellow–blue, white–black (see Eq. 1). Consequently, in the context of this paper Eq. 2 *is* to be understood as claiming that the color $\boldsymbol{c}$ is perceived as a weighted average of the phenomenal attributes of the color addends $\boldsymbol{c}_1$and $\boldsymbol{c}_2$. That such an interpretation of Eq. 2 is tenable was conclusively shown by Hurvich and Jameson (1957). Their seminal hue-cancellation experiments allowed them to assign different relative amounts of Hering's phenomenal attributes to each wavelength in the visual spectrum ('chromatic valence'). The *appearance* of any color mixture could then be predicted using Eq. 2 (see details in Hurvich & Jameson, 1957, pp. 388–392).

pure unique red to pure unique yellow (see the vector $\boldsymbol{c}$ in Fig. 1). Notice that this orange will not be pure since it will contain some grayness. Hering himself seems to have avoided this problem by using the color equation: $c + w + s = 1$, where c is the amount chromaticness in a color sensation, w is the amount of whiteness, and s is the amount of blackness (Hård et al., 1996; Kuehni, 2003, chapter 2). When $w = s = 0$, this equation does give a hue circle with radius 1. Using this equation, leads to a color space whose shape is that of a double cone (which is indeed the shape of the NCS color space; see details in Hård et al., 1996). There are two problems with Hering's color equation: (a) it does not treat the achromatic elementary colors as part of an opponent pair, which is inconsistent with Hering's own proposal of three opponent pairs (Hurvich & Jameson, 1957; for a discussion of Hering's inconsistency on the issue of the achromatic processes, see Werner et al., 1984); (b) it is not consistent with the existence of two *separate* chromatic mechanisms because arithmetic rather than vectorial addition is used to arrive at c (see Eq. 2 in Hård et al., 1996).[3] Some of Hering's followers did, however, seem to take his observations to their logical conclusion and constructed color spaces that have the shape of a double pyramid: Höfler, at the end of the 19th century, suggested a double-square pyramid color space (see Fig. 2-36 in Kuehni, 2003); at the turn of the 20th century, Ebbinghaus and Titchener (separately) suggested tilted double pyramids (see Figs. 2-38 and 2-39 in Kuehni, 2003). Since the term hue circle has become so ubiquitous in discussions of color science, I currently ignore this apparent

---

[3] As a consequence, the NCS must keep track of another variable, ϕ, which indicates the polar angle of the hue sensation.

inconsistency in Hering's thinking and continue to use the term in the discussion that follows. In addition, a hue circle is shown in the Heringian scheme of phenomenal color space of Fig. 1.

Neurophysiological evidence from monkey retinal ganglion cells (De Monasterio et al., 1975; Gouras, 1968) and lateral geniculate nucleus cells (which are fed by the ganglion cells) (Derrington et al., 1984; De Valois et al., 1967) shows that they receive excitatory and inhibitory inputs from various combinations of the long-wavelengths cones (L-cones), medium-wavelengths cones (M-cones), and short-wavelengths cones (S-cones). These so-called 'opponent cells' were therefore initially thought to be the neurophysiological instantiation of Hering's opponent-processes mechanisms. For example, cells that receive excitatory inputs from L-cones and inhibitory inputs from M-cones (often colloquially referred to as $(L - M)$-cells) were suggested to be the neural implementation of Hering's red–green mechanism. However, it gradually became clear that the zero crossings in the responses of these cells to spectral colors did not correspond to the spectral locations of the unique hues, thus precluding them from being an instantiation of Hering's mechanisms (Broackes, 2011; Valberg, 2001; Webster et al., 2000). The response patterns of color-sensitive cells in the visual cortex also fail to show the properties required to be behind Hering's opponent-processes mechanisms (Bohon et al., 2016; Lennie et al., 1990; Mollon, 2009). All in all, the neurophysiological mechanisms that presumably give rise to the three perceptual channels of opponent processes and to the six elementary color sensations are still unknown (Forder et al., 2017; Mollon, 2006, 2009).

Another indication that opponent cells cannot account for Hering's opponent-processes mechanisms comes from dichromats, namely, people who have only two types of functional cones (Sharpe et al., 1999). On the hypothesis that $(L-M)$-cells are the neural implementation of Hering's red–green mechanism, the absence of L-cones (in the case of protanopia) or M-cones (in the case of deuteranopia) should lead to the vanishing of red and green percepts. Consequently, such dichromats should presumably only perceive hues along the yellow–blue axis. This indeed is the standard view (Byrne & Hilbert, 2010; see illustration in Fig. 1.13 of Sharpe et al., 1999). However, as the thorough review, analysis, and meta-analysis by Broackes (2010) conclusively shows, there is a plethora of evidence to contradict this consensual view. Specifically, when the size of the stimulus is large, when the chromatic saturation of the stimulus is high, and when the illumination is not restrictive, there is hardly any doubt that dichromats do perceive green and red (this was shown on rare individuals who have one eye that is normal and one eye that is dichromatic) (*ibid*.). Thus, in contrast to the prediction of the opponent-cells theory, the absence of either L- or M-cones does not lead to the disappearance of red and green. A similar conclusion is reached for the third kind of dichromats, namely, those people who lack the S-cone (tritanopes). On the opponent-cells hypothesis, Hering's yellow–blue mechanism is instantiated by $\left((L+M)-S\right)$-cells. In tritanopes we would therefore expect the perception of yellow and blue to vanish. This is emphatically *not* the case (reviewed in Mollon, 1982; note that Mollon's review includes so-called 'foveolar tritanopes', who are normal observers that are brought to a tritanopia-like state through the usage of color stimuli that are restricted to the fovea, where S-cones are absent or extremely rare). The fact that tritanopes perceive blue and shades of yellow was dubbed 'the tritanopic paradox' by Mollon. As an important aside, notice that the evidence discussed above indicates that *the phenomenal color space of dichromats is three-dimensional, even though their input is only from two types of cones*. This remarkable and counterintuitive fact might be at the root of the strong opposition among many researchers to the notion that protanopes and deuteranopes perceive red and green, despite the large body of evidence that supports this notion (Broackes, 2010). Interestingly, in the case of monochromats, i.e., people who have only a single type of photoreceptor functioning (either a single type of cones or rods), the phenomenal color space does—as expected—collapse to a one-dimensional phenomenal attribute, which is the axis of lightness (Nordby, 1990; Sharpe et al., 1999). That is, in this case the dimensionality of phenomenal color space does not exceed that of the input.

The discussion so far has left out a fourth phenomenal attribute of color—that of brightness, which is the perceived intensity of a color (Shevell, 2003). Phenomenally, brightness varies from very dim to dazzling. Overall, then, color is *a four-dimensional* phenomenon: the full description of a color percept consists of its red–green, yellow–blue, white–black components *and* its brightness level. Evidently, lightness and brightness are totally distinct phenomenal attributes: lightness is an attribute that varies from black to white, brightness is an attribute that varies from dim to dazzling (Gilchrist, 2007). However, there are indications that the two attributes are related. When an achromatic color is viewed in isolation, namely, when there are no other colors in the field of view (this is called the *unrelated* mode of color presentation), the color is perceived as white (Shevell, 2003). This is because the sensation of black disappears in the unrelated mode of color presentation[4] and consequently so does the sensation of gray. Hence, when the brightness of an unrelated achromatic color is varied, the evoked sensation is of white at different levels of intensity (*ibid*.). Gilchrist (2006, chapter 9) has shown that the same phenomenon occurs for a *related* achromatic color (i.e., an achromatic color viewed in the vicinity of other colors) once the color's luminance (i.e., its absolute light intensity) crosses a certain threshold. His conclusion was that lightness and brightness—although phenomenally distinct—share *a single dimension* (*ibid.*; see his Fig. 9.18). Indeed, it is common in the literature to see a scheme of phenomenal color space where lightness and brightness share the same dimension (e.g., Palmer, 1999, p. 114; Purves & Yegappan, 2017) or to read statements such as 'Lightness can be understood as relative brightness' (Kuehni, 2003, p. 371). This suspected affinity between lightness and brightness is probably behind the common confusion between these two phenomenal attributes and the common (yet erroneous) referral to color as a three-dimensional rather than a four-dimensional phenomenon. A final piece of

[4] The sensation of black cannot be evoked directly by a light stimulus; it only arises when the luminance of a stimulus (i.e., its absolute light intensity) is very much lower than its surroundings (Hurvich & Jameson, 1957; Shevell, 2003).

evidence that points at some relationship between lightness and brightness is that in monochromats the surviving phenomenal attributes of color are lightness and brightness (Nordby, 1990).

What brings about these phenomenal properties of our color experience? Specifically, following are nine basic questions about these properties whose answers are currently unknown:

1. Why are color percepts four-dimensional?
2. What are the mechanisms that instantiate the three perceptual channels of opponent colors? (As we have seen, neurophysiology hasn't found these mechanisms.)
3. Why do the outputs of the three color mechanisms fall into two phenomenally distinct groups (one achromatic, the other chromatic)? Or, looked at from a different perspective, why is it that the outputs of two of the three color mechanisms share a common phenomenal attribute (hue)?
4. Why are there four unique hues? (Recall that neurophysiology hasn't found the neural correlates of these hues.)
5. Why is it that the gamut of all hues can be ordered in a closed continuum? To quote Shepard (1994, p. 17), 'what in the world is the source… of the circularity, discovered by Newton, in the continuum of hues? For this circularity presents us with the psychophysical puzzle that the hues corresponding to the most widely

separated of the visible physical wavelengths, namely red and violet, appear more similar to each other than either does to a hue of intermediate wavelength, such as green.'

6. Why is it that white and black, i.e., the two achromatic opponent colors, can perceptually coexist in one color, but the two elementary colors of each of the chromatic opponent pairs are mutually exclusive?
7. Why do colors additively mix according to the center of gravity principle (Eq. 2)?
8. How is it that the phenomenal color space of dichromats is three-dimensional? Why, then, is the phenomenal color space of monochromats only one-dimensional and restricted to lightness?
9. What is the nature of the relationship between lightness and brightness? Do they indeed share a single dimension?

Several of these intriguing questions have been addressed in the past. Much attention has been given to the question of why there exist four unique hues. Many (e.g., Broackes, 2011; Mollon, 2006; Shepard, 1992, 1994) have speculated that the evolution of four unique hues may be attributed to an adaptation to the illumination characteristics of our natural environment (e.g., the spectrum of illumination brought about by sunlight and skylight). Mollon (2006) suggested that similar factors can also explain the existence of white as an elementary color. In contrast to these suggestions, Valberg (2001) concluded that 'The structuring of colour perception imposed by the unique hues does not seem to us today to have an obvious physical or environmental cause. Neither do these hues have any behavioural importance…' (p. 1654). Purves et al. (2000) hypothesized that the four unique hues arose as a solution to a 'four-color-map problem' that the two-dimensional retinal sheet presumably imposes on the visual system. Purves and Yegappan (2017) extended these ideas and proposed that the geometrical demands that the two-dimensional retinal sheet makes on the visual system can also explain the fact that the hue gamut can be continuously ordered in a circle. Tackling the riddle of how dichromats perceive a three-dimensional color space, Broackes (2010) suggested that 'seeing a surface color *under two different illuminants* [might] provide a dichromat, who at first seemed to lack information on the red-green dimension, with information about that dimension' (p. 337; italics in the original).

Here I try to answer the questions regarding the source of the phenomenal properties of color experience by taking a very different approach from the evolutionary, ecological, and neurophysiological approaches of past studies. My starting point is the dual-aspect theory of phenomenal consciousness. This theory, which can be interpreted in either monistic or dualistic terms (Stubenberg, 2018, section 8.3), suggests that one or more entities in our universe have, in addition to their objective aspects, dual aspects that are subjective and phenomenal (see, e.g., Chalmers, 1996, chapter 8). On the dual-aspect theory, it makes sense to expect a precise correspondence between a system's phenomenal states and the objective states of its underlying physical (or functional) substrate (Chalmers, 1996, chapters 6 and 8; Cortês et al., 2021; Lockwood, 1989, chapter 11). Here, for example, is Lockwood:

> Take some range of phenomenal qualities. Assume that these qualities can be arranged according to some abstract n-dimensional space, in a way that is faithful to their perceived similarities and degrees of similarities... Then my… proposal is that there exists, within the brain, some physical system, the states of which can be arranged in some n-dimensional state space… And the two states are to be equated with each other: the phenomenal qualities are identical with the states of the corresponding physical system.
>
> (1989, p. 172)

In this paper I identify such a physical system for the case of color experience. I show that the phenomenal properties of our color experience have exact analogs in the mathematical properties of qubit mixed states reconstructed through quantum state tomography. Based in this result I conjecture that color experience is the phenomenal dual aspect of an ensemble of qubits undergoing quantum state tomography somewhere in the brain.

The paper has the following structure. In Section 2 I review qubits, their Bloch-space representation, and qubit quantum state tomography. Section 2 does not contain any original contribution, but it provides the necessary background for the main argument of this paper, which is presented in Section 3. In that section I lay out the analogs between the phenomenal properties of color percepts and the mathematical properties of qubit states reconstructed through quantum state tomography. Based on these analogs I suggest that the former are phenomenal dual aspects of the latter. Section 4 is dedicated to a discussion.

2. Qubits, their Bloch-space representation, and quantum state tomography

2.1 Pure states and their Bloch-sphere representation

Two-state quantum systems, which in the field of quantum computation are often referred to as *qubits*, are systems that can exist in a superposition of two physically distinguishable states. Some common examples of qubit systems are the spin state of spin-1/2 particles, the polarization state of photons, and atomic systems that can be approximated as effectively having only two electronic levels (Altepeter et al., 2004). I will represent the two states of a qubit by the Hilbert-space vectors $|\pm\rangle$. These two vectors are orthogonal and therefore constitute a basis for the two-dimensional Hilbert space that they inhibit. A qubit is then fully described by a state vector, denoted $|\psi\rangle$, given by the following superposition:

$$|\psi\rangle = \cos\frac{\theta}{2} e^{i\phi_\alpha}|+\rangle + \sin\frac{\theta}{2} e^{i\phi_\beta}|-\rangle, \tag{3}$$

where $0 \leq \theta \leq \pi$, $0 \leq \phi_\alpha, \phi_\beta \leq 2\pi$ (Blum, 1981, chapter 1). Since two-dimensional Hilbert space is isomorphic to $\mathbb{C}^2$, it has become customary to ignore mathematical niceties and treat the state vector $|\psi\rangle$ as if it was the vector $\left(\cos\frac{\theta}{2} e^{i\phi_\alpha}, \sin\frac{\theta}{2} e^{i\phi_\beta}\right)^{\mathrm{T}}$ in $\mathbb{C}^2$ (e.g., Aerts & Sassoli de Bianchi, 2017; Blum, 1981, chapter 1). I will follow suit.

Because the global phase of a quantum state does not have any observational effect, all the qubit states $e^{i\lambda}|\psi\rangle$, $\lambda \in \mathbb{R}$, are observationally identical (Blum, 1981, chapter 1). Clearly, it would be much more efficient to have a representation that condenses all the qubit states $e^{i\lambda}|\psi\rangle$, $\lambda \in \mathbb{R}$, into a single mathematical entity. The density-operator representation of quantum states,

$$\rho = |\psi\rangle\langle\psi|, \tag{4}$$

where $\langle\psi| = (|\psi\rangle^*)^{\mathrm{T}} \equiv |\psi\rangle^{\dagger}$, which is an alternative to the state-vector representation of Eq. 3 (*ibid*.), provides us with exactly such an entity because $e^{i\lambda}|\psi\rangle\langle\psi|e^{-i\lambda} = |\psi\rangle\langle\psi| = \rho$. Substituting the expression for $|\psi\rangle$ in Eq. 3 into Eq. 4 (or, for that matter, substituting $e^{i\lambda}|\psi\rangle$ into Eq. 4) and using a couple of basic trigonometric identities we obtain the following matrix representation for the density operator:

$$\rho = \frac{1}{2}\begin{bmatrix} 1+\cos\theta & \sin\theta\, e^{-i} \\ \sin\theta\, e^{i\phi} & 1-\cos\theta \end{bmatrix}, \tag{5}$$

where $\phi = \phi_\beta - \phi_\alpha$. It is easy to see that the expression for ρ in Eq. 5 is isomorphic to the following unit vector in $\mathbb{R} \times \mathbb{C}$:

$$\widehat{\boldsymbol{b}} = \left(\cos\theta\,, \sin\theta\, e^{i\phi}\right)^{\mathrm{T}} = \sin\theta\cos\phi\,\widehat{\boldsymbol{x}}_1 + \sin\theta\sin\phi\,\widehat{\boldsymbol{x}}_2 + \cos\theta\,\widehat{\boldsymbol{x}}_3\,, \tag{6}$$

where $\widehat{\boldsymbol{x}}_1 = (0,1)^{\mathrm{T}}$, $\widehat{\boldsymbol{x}}_2 = (0,i)^{\mathrm{T}}$, $\widehat{\boldsymbol{x}}_3 = (1,0)^{\mathrm{T}}$ (Aerts & Sassoli de Bianchi, 2017). Notice that the loss of the global phase $e^{i\lambda}$ in the transition from the state vector $e^{i\lambda}|\psi\rangle$ to the density operator ρ manifests itself in the transition of the representation from $\mathbb{C}^2$ to $\mathbb{R} \times \mathbb{C}$.[5]

If we interpret the parameters θ and ϕ in Eq. 6 as the inclination and azimuthal angles of a spherical coordinate system ($0 \leq \theta \leq \pi$, $0 \leq \phi \leq 2\pi$) , we see that $\hat{\boldsymbol{b}}$ provides us with a geometrical representation of the Hilbert-space vector $|\psi\rangle$ (more precisely, a geometrical representation of *all* Hilbert space vectors $e^{i\lambda}|\psi\rangle$, $\lambda \in \mathbb{R}$). The unit vector $\hat{\boldsymbol{b}}$ is commonly referred to as the Bloch vector. The set of all possible Bloch vectors (created by taking all possible values of θ and ϕ in Eq. 6) defines a unit sphere known as the Bloch (or Poincaré) sphere (Aerts & Sassoli de Bianchi, 2017; Altepeter et al., 2004). Figure 2 gives a schematic description of the Bloch sphere and one example of a Bloch vector. The $\mathbb{R} \times \mathbb{C}$ space in which the Bloch vectors exist is an abstract space called the Bloch space.

[5] In the literature it is more common to represent $\hat{\boldsymbol{b}}$ as a vector in $\mathbb{R}^3$ rather than in $\mathbb{R} \times \mathbb{C}$ (e.g., Aerts & Sassoli de Bianchi, 2017). However, I contend that the representation in $\mathbb{R} \times \mathbb{C}$ is the correct one because, unlike the $\mathbb{R}^3$ representation, it retains the roots of $\hat{\boldsymbol{b}}$ in $\mathbb{C}^2$.

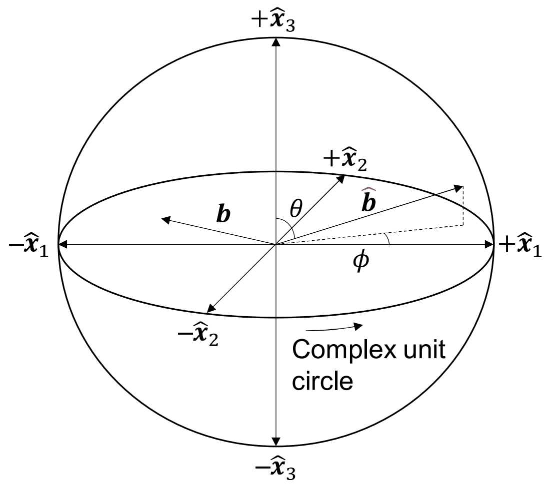

Figure 2. The Bloch sphere/ball. All vectors on the surface of this unit sphere represent qubit pure states. One example is shown in the figure: the vector $\hat{\boldsymbol{b}}$, whose inclination angle is θ and whose azimuthal angle is ϕ The six unit vectors $\pm\hat{\boldsymbol{x}}_i \in \mathbb{R} \times \mathbb{C}$, $i = 1, 2, 3$, are the Bloch-space representation of the Hilbert-space vectors $|\pm\hat{\boldsymbol{x}}_i\rangle$ (see text for details). The vectors $\pm\hat{\boldsymbol{x}}_1$, $\pm\hat{\boldsymbol{x}}_2$ reside on the complex unit circle in Bloch space. All vectors inside the Bloch sphere represent qubit mixed states. The vector $\boldsymbol{b}$ shown in the figure ($\|\boldsymbol{b}\| < 1$) is an example of such a mixed state.

From Eq. 3 and Eq. 6 it is easy to confirm that the unit vectors $\pm\hat{\boldsymbol{x}}_3$ are the Bloch-space representations of the Hilbert-space basis vectors $|\pm\rangle$. Therefore, from now one I will write $|\pm\hat{\boldsymbol{x}}_3\rangle$ instead of $|\pm\rangle$. Similarly, it can readily be shown that the unit vectors $\pm\hat{\boldsymbol{x}}_1$ and $\pm\hat{\boldsymbol{x}}_2$ in Bloch space correspond to the following Hilbert-space state vectors:

$$|\pm\hat{\boldsymbol{x}}_1\rangle = \frac{1}{\sqrt{2}}(|+\hat{\boldsymbol{x}}_3\rangle \pm |-\hat{\boldsymbol{x}}_3\rangle), \tag{7a}$$

$$|\pm\hat{\boldsymbol{x}}_2\rangle = \frac{1}{\sqrt{2}}(|+\hat{\boldsymbol{x}}_3\rangle \pm i|-\hat{\boldsymbol{x}}_3\rangle). \tag{7b}$$

2.2 The Pauli operators

The three operators that obey the following eigenvector/eigenvalue equations

$$\sigma_i|\pm\hat{\boldsymbol{x}}_i\rangle = \pm|\pm\hat{\boldsymbol{x}}_i\rangle, \tag{8}$$

$i = 1, 2, 3$, are called the Pauli operators. (Notice, then, that the vectors $\pm\hat{\boldsymbol{x}}_i$, $i = 1, 2, 3$, are the Bloch-space representations of the Hilbert-space vectors that are the eigenvectors of the Pauli operator σ_i.) In the literature it is very common to represent the Pauli operators as matrices relative to the $|\pm\hat{\boldsymbol{x}}_3\rangle$ basis. The result, known as the standard matrix representation of the Pauli operators, is given by

$$\sigma_1 = \begin{bmatrix} 0 & 1 \\ 1 & 0 \end{bmatrix}, \sigma_2 = \begin{bmatrix} 0 & -i \\ i & 0 \end{bmatrix}, \sigma_3 = \begin{bmatrix} 1 & 0 \\ 0 & -1 \end{bmatrix}. \tag{9}$$

Given the eigenvectors and eigenvalues of σ_i in Eq. 8, we can employ the eigenvalue decomposition theorem to obtain an explicit expression for σ_i:

$$\sigma_i = |+\hat{\boldsymbol{x}}_i\rangle\langle+\hat{\boldsymbol{x}}_i| - |-\hat{\boldsymbol{x}}_i\rangle\langle-\hat{\boldsymbol{x}}_i|, \tag{10}$$

$i = 1, 2, 3$. Equation 10 shows that each Pauli operator σ_i, $i = 1, 2, 3$, is composed of two underlying operators that operate in an *antagonistic* manner: $|+\hat{\boldsymbol{x}}_i\rangle\langle+\hat{\boldsymbol{x}}_i|$ and $|-\hat{\boldsymbol{x}}_i\rangle\langle-\hat{\boldsymbol{x}}_i|$.

It can easily be shown (e.g., from Eq. 9) that the Pauli operators are Hermitian, i.e., $\sigma_i = \sigma_i^\dagger$, $i = 1, 2, 3$, and are therefore quantum observables (Blum, 1981, chapter 1). Hence, the physical content of Eq. 8 is that immediately after a measurement of the observable σ_i, the measured system will be projected into the state $|+\hat{\boldsymbol{x}}_i\rangle$ or into the state $|-\hat{\boldsymbol{x}}_i\rangle$. The set $\{\mathbb{I}, \sigma_1, \sigma_2, \sigma_3\}$, where $\mathbb{I}$ is the identity operator, constitutes an orthogonal basis for the vector space of linear operators acting on two-dimensional Hilbert space (Bertlmann & Krammer, 2008). I will refer to this basis as the Pauli basis. It spans the space of all observables of two-state quantum systems. Since the identity operator in two-dimensional Hilbert space belongs to the Pauli basis, it is often referred to as the *zeroth* Pauli operator, σ_0. We can use the eigenvalue decomposition theorem to express the identity operator in the following manner:

$$\mathbb{I} = \sigma_0 = |+\hat{\boldsymbol{n}}\rangle\langle+\hat{\boldsymbol{n}}| + |-\hat{\boldsymbol{n}}\rangle\langle-\hat{\boldsymbol{n}}|, \tag{11}$$

where $|+\hat{\boldsymbol{n}}\rangle$ and $|-\hat{\boldsymbol{n}}\rangle$ are any two orthogonal unit vectors in two-dimensional Hilbert space (for example, $|+\hat{\boldsymbol{x}}_i\rangle$ and $|-\hat{\boldsymbol{x}}_i\rangle$, $i = 1, 2, 3$). Equation 11 is often referred to as the *completeness relation*.

2.3 Mixed states and their Bloch-ball representation

Quantum systems that can be described by a state vector (e.g., Eq. 3) are said to be in a *pure state*. However, quantum systems can also exist in a *mixed state* (Blum, 1981, chapter 2). Mixed states (or *mixtures*) arise when there is an ensemble of quantum systems where each is in a pure state, but the *phase* of each of these pure states does not affect the observational properties of the ensemble. That is, the states of the constituent systems do not *interfere* with each other. (By contrast, when the constituent systems do interfere with each other, the ensemble as whole is in a pure state.) Mathematically, mixed states are described by an extension of the density operator that we met in Eq. 4 above:

$$\rho = \sum_k W_k\, |\psi_k\rangle\langle\psi_k|, \tag{12}$$

where k goes over the different pure states in the ensemble, $|\psi_k\rangle$ is the kth pure state in the ensemble, and W_k is the relative weight of this pure state (i.e., the ratio between the number of particles in the kth pure state and the total number of particles in the ensemble) (*ibid*.). Thus, $0 < W_k \leq 1$ and $\sum_k W_k = 1$. The expression for the density operator in Eq. 12 elegantly captures the fact that a mixture is a statistical average of quantum systems in a pure state that do not interfere with each other. It can be shown that the density operator is Hermitian and is therefore a quantum observable (*ibid*.). A second physical situation where mixed states arise when there is a composite quantum system that consists of several subsystems (Altepeter et al., 2004). Each of the subsystems is then in a mixed state because the entanglement prevents the phase of the subsystem from affecting the results of observations on it.

Here we will be only interested in density operators that describe qubit mixed states. It can be shown that the density operator for qubits can always be written as the following linear combination of the Pauli operators:

$$\rho = \frac{1}{2}(\mathbb{I} + b_1\sigma_1 + b_2\sigma_2 + b_3\sigma_3), \tag{13}$$

where $b_1, b_2, b_3 \in \mathbb{R}$ and ${b_1}^2 + {b_2}^2 + {b_3}^2 \leq 1$ (Blum, 1981, chapter 1). If we look at the density operator ρ in Eq. 13 as a vector in the linear space of Hermitian operators, we see that the $\mathbb{R} \times \mathbb{C}$ vector

$$\boldsymbol{b} = (b_3, b_1 + ib_2)^{\mathrm{T}} = b_1\widehat{\boldsymbol{x}}_1 + b_2\widehat{\boldsymbol{x}}_2 + b_3\widehat{\boldsymbol{x}}_3 \tag{14}$$

($\widehat{\boldsymbol{x}}_1$, $\widehat{\boldsymbol{x}}_2$, and $\widehat{\boldsymbol{x}}_3$ are defined as in Eq. 6) can be taken as its *coordinate vector* relative to the Pauli basis.[6] Hence, there is a one-to-one correspondence between the density operators of qubits and the set of vectors $\boldsymbol{b}$. The fact that $\boldsymbol{b} \in \mathbb{R} \times \mathbb{C}$ reflects the loss of the phase of each of the pure states comprising the mixture (see the discussion related to Eq. 6 and its footnote). From the constraint ${b_1}^2 + {b_2}^2 + {b_3}^2 \leq 1$ on Eq. 13, we see that $\|\boldsymbol{b}\| \leq 1$ and conclude that the set of vectors $\boldsymbol{b}$ fills the entire volume of the Bloch sphere of Fig. 2, i.e., these vectors constitute the Bloch ball. Thus, the vector $\boldsymbol{b}$ is a generalization of the unit Bloch vector $\widehat{\boldsymbol{b}}$ of Eq. 6. It is therefore referred to as the Bloch vector representing the density operator ρ (one example is shown in Fig. 2). As we saw in Section 2.1, when $\|\boldsymbol{b}\| = 1$ the Bloch vector lies on the surface of the Bloch sphere and hence represents a pure state.

As can be easily verified using Eq. 12, when two qubit mixtures (i.e., two qubit ensembles in a mixed state) are combined, the resulting mixture is represented by a Bloch vector that is a weighted average of the Bloch vectors of the addends. For example, if one mixture, represented by the Bloch vector $\boldsymbol{b}_1$, contains N_1 qubits, and a second mixture, represented by the Bloch vector $\boldsymbol{b}_2$, contains N_2 qubits, the Bloch-vector representation of the resultant mixture is given by

$$\boldsymbol{b} = \frac{N_1}{N_1 + N_2}\boldsymbol{b}_1 + \frac{N_2}{N_1 + N_2}\boldsymbol{b}_2. \tag{15}$$

[6] This representation omits the uninteresting constant coefficient of the identity operator in Eq. 13.

Any measurement on a mixture is associated with some observable O. A measurement of O projects each qubit in the mixture into one of its two eigenstates. The density operator can give us the probability of obtaining each of the eigenstates (Altepeter et al., 2004). Using these probabilities we can calculate the expectation value (i.e., mean value) of the measurement results of operating with O on the mixture. This value, denoted $\langle O \rangle$, is given by $\mathrm{tr}(\rho O)$, where $\mathrm{tr}()$ is the trace operation and ρ is the mixture's density operator (Blum, 1981, chapter 2). Using the expression for ρ in Eq. 13 and taking the observable to be any one of the Pauli observables, σ_i, $i = 1, 2, 3$, this formula yields

$$b_i = \langle \sigma_i \rangle \tag{16}$$

(Bertlmann & Krammer, 2008). An immediate conclusion from Eq. 16 is that the Bloch vector of Eq. 14 is given by

$$\boldsymbol{b} = (\langle \sigma_3 \rangle, \langle \sigma_1 \rangle + i\langle \sigma_2 \rangle)^{\mathrm{T}} = \langle \sigma_1 \rangle \hat{\boldsymbol{x}}_1 + \langle \sigma_2 \rangle \hat{\boldsymbol{x}}_2 + \langle \sigma_3 \rangle \hat{\boldsymbol{x}}_3. \tag{17}$$

2.4 Qubit quantum state tomography

Suppose that we have an ensemble of qubits whose unknown mixed state we wish to determine. Relative to some *specific* Pauli basis of observables, the mixture's density operator ρ is given by some specific set of values of b_i, $i = 1, 2, 3$, in Eq. 13. To determine the mixture's density operator (or, equivalently, determine its Bloch vector), we see from Eq. 16 (or from Eq. 17) that we need to measure the expectation values of the three Pauli observables in the chosen basis. This process of reconstructing a mixture's quantum state is called *qubit quantum state tomography* (Altepeter et al., 2004). Notice that to carry out qubit quantum state tomography (QQST) it is required that we choose a specific Pauli basis of observables. How do we do that? A related question is: once we chose such a basis, what are the physical operations that we need to carry out to measure each of the Pauli observables in the triad? This section answers these two questions.

Equation 10 shows that the three Pauli observables are constructed through the six Hilbert-space vectors $|\pm\hat{\boldsymbol{x}}_i\rangle$, $i = 1, 2, 3$. Since we defined the Hilbert-space vectors $|\pm\hat{\boldsymbol{x}}_1\rangle$ and $|\pm\hat{\boldsymbol{x}}_2\rangle$ as linear combinations of the vectors $|\pm\hat{\boldsymbol{x}}_3\rangle$ (see Eq. 7), we conclude that choosing a specific Pauli basis of observables boils down to (a) choosing a specific basis for two-dimensional Hilbert space, and then (b) using this basis to construct the four Hilbert-space vectors specified in Eq. 7.

Next, how do we operationally obtain the expectation values of the Pauli observables in the specific Pauli basis that we chose? From Eq. 10 it follows that

$$\langle \sigma_i \rangle = \langle |+\hat{\boldsymbol{x}}_i\rangle\langle +\hat{\boldsymbol{x}}_i| \rangle - \langle |-\hat{\boldsymbol{x}}_i\rangle\langle -\hat{\boldsymbol{x}}_i| \rangle, \tag{18}$$

$i = 1, 2, 3$. The expectation value $\langle |+\hat{\boldsymbol{x}}_i\rangle\langle +\hat{\boldsymbol{x}}_i| \rangle$ gives the probability of projecting a mixed state into the state $|+\hat{\boldsymbol{x}}_i\rangle$, $i = 1, 2, 3$ (*ibid.*). Similarly, the expectation value $\langle |-\hat{\boldsymbol{x}}_i\rangle\langle -\hat{\boldsymbol{x}}_i| \rangle$ gives the probability of projecting a mixed state into the state $|-\hat{\boldsymbol{x}}_i\rangle$, $i = 1, 2, 3$. Thus, Eq. 18 provides us with the answer to the question of how to find the expectation values of the Pauli observables of the specific Pauli basis that we chose: for each of the pair of states $|+\hat{\boldsymbol{x}}_i\rangle$ and $|-\hat{\boldsymbol{x}}_i\rangle$, $i = 1, 2, 3$, we (a) conduct an experiment that measures the probability of projecting the mixed state into the state $|+\hat{\boldsymbol{x}}_i\rangle$; (b) conduct an experiment that measures the probability of projecting the mixed state into the state $|-\hat{\boldsymbol{x}}_i\rangle$; (c) subtract the two probabilities. Notice, then, that QQST is a serial process because each of the measurements mentioned above is performed separately. Since each measurement changes the state of the mixture (projecting it into two orthogonal states; see previous section), we must have several identical copies of the mixture to carry out a complete QQST (*ibid*.).

Actual experiments on a qubit mixture do not obtain the expectation values $\langle|\pm\hat{\boldsymbol{x}}_i\rangle\langle\pm\hat{\boldsymbol{x}}_i|\rangle$, $i = 1, 2, 3$, in Eq. 18 in terms of probabilities, but rather in terms of numbers of qubits in the mixture. To obtain the results in terms of probabilities, we need to first measure the overall number of qubits in the mixture (this number is often referred to as the mixture's intensity; see Blum, 1981, chapter 1) and then use this number to normalize our expectation values. For clarity, it will be convenient to explicitly distinguish between the 'raw', unnormalized expectation values and the normalized ones, which are related in the following way:

$$\langle|\pm\hat{\boldsymbol{x}}_i\rangle\langle\pm\hat{\boldsymbol{x}}_i|\rangle = \frac{\langle|\pm\hat{\boldsymbol{x}}_i\rangle\langle\pm\hat{\boldsymbol{x}}_i|\rangle_{\mathrm{u}}}{N}, \tag{19}$$

$i = 1, 2, 3$, where N is the number of qubits in the mixture and the subscript on the expectation value on the right-hand side indicates that this is an unnormalized expectation value. Substituting Eq. 19 into Eq. 18 we find that $\langle\sigma_i\rangle = \langle\sigma_i\rangle_{\mathrm{u}}/N$, $i = 1, 2, 3$. We therefore see that to complete QQST we need an additional measurement to the ones discussed above—one that counts the overall number of qubits in the mixture

(Blum, 1981, chapter 1). However, instead of conducting this measurement as a separate process, we can obtain the number of qubits in the mixture by simply summing the number of qubits in found in the states $|+\hat{\boldsymbol{x}}_i\rangle$ and $|-\hat{\boldsymbol{x}}_i\rangle$ *for one of the values* $i = 1, 2, 3$. Since we chose $|\pm\hat{\boldsymbol{x}}_3\rangle$ as our basis of two-dimensional Hilbert space, it makes sense to use this pair to obtain the number of qubits in the mixture. We can express this counting process using the completeness relation of Eq. 11 in the following way:

$$N = \langle\sigma_0\rangle_{\mathrm{u}} = \langle|+\hat{\boldsymbol{x}}_3\rangle\langle+\hat{\boldsymbol{x}}_3|\rangle_{\mathrm{u}} + \langle|-\hat{\boldsymbol{x}}_3\rangle\langle-\hat{\boldsymbol{x}}_3|\rangle_{\mathrm{u}}. \tag{20}$$

Notice that once we measured the pair $\langle|\pm\hat{\boldsymbol{x}}_3\rangle\langle\pm\hat{\boldsymbol{x}}_3|\rangle_{\mathrm{u}}$, we only need to measure *one* expectation value from the pair $\langle|\pm\hat{\boldsymbol{x}}_1\rangle\langle\pm\hat{\boldsymbol{x}}_1|\rangle_{\mathrm{u}}$ and *one* expectation value from the pair $\langle|\pm\hat{\boldsymbol{x}}_2\rangle\langle\pm\hat{\boldsymbol{x}}_2|\rangle_{\mathrm{u}}$ to complete the QQST process. This is because the sum in each pair of expectation values is N, a number that we already obtained from the measurements specified in Eq. 20. Overall, then, QQST requires only *four* measurements rather than the six implicit in Eq. 18. It is easy to show that this equation can now be simplified to

$$\langle\sigma_1\rangle = \langle|+\hat{\boldsymbol{x}}_1\rangle\langle+\hat{\boldsymbol{x}}_1|\rangle - (1 - \langle|+\hat{\boldsymbol{x}}_1\rangle\langle+\hat{\boldsymbol{x}}_1|\rangle), \tag{21a}$$

$$\langle\sigma_2\rangle = (1 - \langle|-\hat{\boldsymbol{x}}_2\rangle\langle-\hat{\boldsymbol{x}}_2|\rangle) - \langle|-\hat{\boldsymbol{x}}_2\rangle\langle-\hat{\boldsymbol{x}}_2|\rangle, \tag{21b}$$

$$\langle\sigma_3\rangle = \langle|+\hat{\boldsymbol{x}}_3\rangle\langle+\hat{\boldsymbol{x}}_3|\rangle - \langle|-\hat{\boldsymbol{x}}_3\rangle\langle-\hat{\boldsymbol{x}}_3|\rangle, \tag{21c}$$

where we arbitrarily chose to measure the state $|+\hat{\boldsymbol{x}}_1\rangle$ from the pair $|\pm\hat{\boldsymbol{x}}_1\rangle$ and the state $|-\hat{\boldsymbol{x}}_2\rangle$ from the pair $|\pm\hat{\boldsymbol{x}}_2\rangle$.

3. Color percepts are phenomenal dual aspects of qubit mixed states

3.1 The hypothesis

The goal of this section is to convincingly make the case for the following hypothesis:

> H: Color percepts are phenomenal dual aspects of the qubit mixed states reconstructed through quantum state tomography. The *phenomenal* properties of color percepts are determined by the *mathematical* properties of these qubit states.

To support H I will demonstrate that it answers the nine basic questions regarding the phenomenal properties of color experience that were posed in the *Introduction*.

Before we delve into these questions, let us do some preparatory work. Color, as will be recalled from the *Introduction*, is a four-dimensional phenomenon: every color percept can be represented by the tetrad $(Q, \boldsymbol{c})$, where Q is the color's brightness and he vector $\boldsymbol{c}$ is given in Eq. 1. In Section 2.4 it was shown that to fully reconstruct the state of a mixture, QQST requires the measurement of four parameters, which we can aggregate into the tetrad $(N, \boldsymbol{b})$, where N is the number of qubits in the mixture (i.e., the mixture's intensity) and $\boldsymbol{b}$ is the Bloch vector (Eq. 17). The hypothesis H suggests that the phenomenal properties of a color percept $(Q, \boldsymbol{c})$ are dual aspects of the mathematical properties of $(N, \boldsymbol{b})$. In order to be duals of each other, there must exist a one-to-one correspondence (i.e., an isomorphism) between the tetrad $(N, \boldsymbol{b})$ and the tetrad $(Q, \boldsymbol{c})$. Let us unpack this statement. First, the isomorphism between $\boldsymbol{b}$ and $\boldsymbol{c}$ can be expressed in more detail using Eq. 17 and Eq. 1:

$$\boldsymbol{b} = \langle\sigma_1\rangle\hat{\boldsymbol{x}}_1 + \langle\sigma_2\rangle\hat{\boldsymbol{x}}_2 + \langle\sigma_3\rangle\hat{\boldsymbol{x}}_3 \;\leftrightarrow\; \boldsymbol{c} = (R - G)\hat{\boldsymbol{\imath}} + (Y - B)\hat{\boldsymbol{\jmath}} + (W - S)\hat{\boldsymbol{k}}. \qquad (22)$$

Since each color vector is matched to a Bloch vector, phenomenal color space must be isomorphic to Bloch space. This is schematized in Fig. 3.

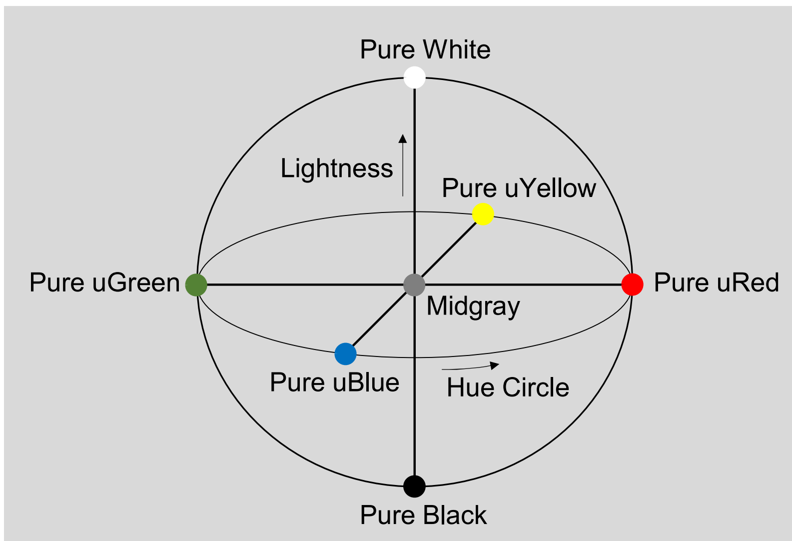

Figure 3. Color space as the phenomenal dual of Bloch space (see Fig. 2). Hering's six basic colors are the phenomenal dual aspect of the unit vectors $\pm\hat{\boldsymbol{x}}_1$, $\pm\hat{\boldsymbol{x}}_2$, $\pm\hat{\boldsymbol{x}}_3$ in Bloch space. The lightness axis in phenomenal color space corresponds to the x_3-axis in Bloch space. The hue circle in phenomenal color space corresponds to the complex unit circle in Bloch space.

Substituting Eq. 18 into the left-hand side of Eq. 22 yields the following component-by-component version of Eq. 22:

$$\langle\sigma_1\rangle = \langle|{+\hat{\boldsymbol{x}}_1}\rangle\langle{+\hat{\boldsymbol{x}}_1}|\rangle - \langle|{-\hat{\boldsymbol{x}}_1}\rangle\langle{-\hat{\boldsymbol{x}}_1}|\rangle \;\leftrightarrow\; R - G, \qquad (23a)$$

$$\langle\sigma_2\rangle = \langle|{+\hat{\boldsymbol{x}}_2}\rangle\langle{+\hat{\boldsymbol{x}}_2}|\rangle - \langle|{-\hat{\boldsymbol{x}}_2}\rangle\langle{-\hat{\boldsymbol{x}}_2}|\rangle \;\leftrightarrow\; Y - B, \qquad (23b)$$

$$\langle\sigma_3\rangle = \langle|{+\hat{\boldsymbol{x}}_3}\rangle\langle{+\hat{\boldsymbol{x}}_3}|\rangle - \langle|{-\hat{\boldsymbol{x}}_3}\rangle\langle{-\hat{\boldsymbol{x}}_3}|\rangle \;\leftrightarrow\; W - S. \qquad (23c)$$

Notice that in Eq. 23 opponent processes in Bloch space correspond to opponent processes in color space (more on this in Section 3.3 below). The correspondence between N and Q completes the isomorphism between $(N, \boldsymbol{b})$ and $(Q, \boldsymbol{c})$. Using Eq. 20 above we can express this correspondence as the fourth component of Eq. 23:

$$N = \langle \sigma_0 \rangle_{\mathrm{u}} = \langle |{+\hat{\boldsymbol{x}}_3}\rangle\langle{+\hat{\boldsymbol{x}}_3}| \rangle_{\mathrm{u}} + \langle |{-\hat{\boldsymbol{x}}_3}\rangle\langle{-\hat{\boldsymbol{x}}_3}| \rangle_{\mathrm{u}} \leftrightarrow Q. \tag{23d}$$

Finally, from a comparison of Figs. 2 and 3 we immediately see that the suggested isomorphism between phenomenal color space and Bloch space means that there is a correspondence between Hering's six elementary color sensations and the six elementary Bloch vectors in Bloch space, i.e., $\pm\hat{\boldsymbol{x}}_i$, $i = 1, 2, 3$:

$$-\hat{\boldsymbol{x}}_1 = (0, -1)^{\mathrm{T}} \leftrightarrow \text{ Pure uGreen,} \qquad +\hat{\boldsymbol{x}}_1 = (0, +1)^{\mathrm{T}} \leftrightarrow \text{ Pure uRed,} \tag{24a}$$

$$-\hat{\boldsymbol{x}}_2 = (0, -i)^{\mathrm{T}} \leftrightarrow \text{ Pure uBlue,} \qquad +\hat{\boldsymbol{x}}_2 = (0, +i)^{\mathrm{T}} \leftrightarrow \text{ Pure uYellow,} \tag{24b}$$

$$-\hat{\boldsymbol{x}}_3 = (-1, 0)^{\mathrm{T}} \leftrightarrow \text{ Pure Black,} \qquad +\hat{\boldsymbol{x}}_3 = (+1, 0)^{\mathrm{T}} \leftrightarrow \text{ Pure White.} \tag{24c}$$

3.2 Preparing the mixture for QQST

The hypothesis H suggests that color percepts are phenomenal dual aspects of qubit mixed states reconstructed through QQST. But how do these mixed states come into being in the first place? It is here that we finally make contact with the physiological machinery of the visual system. I suggest that the role of the complex physiological machinery that has been implicated in the processing of color is *to prepare the qubit mixture* for QQST. More specifically, when a light stimulus strikes a region of the retina, it differentially activates the L-, M-, and S-cones in the region, depending on the spectral composition of the light. The output of the cones then feeds the opponent cells and other color-sensitive cells along the visual pathway. It is suggested that the role of these cells is to ‘encode’, so to speak, a qubit mixture according to the spectral distribution of the light stimulus.

How is this encoding performed? Based on neurophysiological results it commonly assumed that there exist six populations of color-sensitive cells in the early stages of the visual system (see, e.g., Palmer, 1999, chapter 3): $(L-M)$- and $(M-L)$-cells, $\big((L+M)-S\big)$- and $\big(S-(L+M)\big)$-cells, $(L+M+S)$-, and $-(L+M+S)$-cells. A possible scheme for the encoding of the qubit mixture is one where each type of color-sensitive cell creates an ensemble of qubits in a certain mixed state. Here is a specific encoding scheme:

$$(L-M) \longrightarrow I_{\mathrm{r}}\big(\alpha_{\mathrm{r}}\widehat{\boldsymbol{x}}_1 + \beta_{\mathrm{r}}\widehat{\boldsymbol{x}}_2 + \gamma_{\mathrm{r}}(-\widehat{\boldsymbol{x}}_3)\big) \approx I_{\mathrm{r}}\alpha_{\mathrm{r}}\widehat{\boldsymbol{x}}_1, \tag{25a}$$

$$(M-L) \longrightarrow I_{\mathrm{g}}\big(\alpha_{\mathrm{g}}(-\widehat{\boldsymbol{x}}_1) + \beta_{\mathrm{g}}\widehat{\boldsymbol{x}}_2 + \gamma_{\mathrm{g}}\widehat{\boldsymbol{x}}_3\big) \approx I_{\mathrm{g}}\alpha_{\mathrm{g}}(-\widehat{\boldsymbol{x}}_1), \tag{25b}$$

$$\big((L+M)-S\big) \longrightarrow I_{\mathrm{y}}\big(\alpha_{\mathrm{y}}\widehat{\boldsymbol{x}}_1 + \beta_{\mathrm{y}}\widehat{\boldsymbol{x}}_2 + \gamma_{\mathrm{y}}\widehat{\boldsymbol{x}}_3\big) \approx I_{\mathrm{y}}\beta_{\mathrm{y}}\widehat{\boldsymbol{x}}_2, \tag{25c}$$

$$\big(S-(L+M)\big) \longrightarrow I_{\mathrm{b}}\big(\alpha_{\mathrm{b}}(-\widehat{\boldsymbol{x}}_1) + \beta_{\mathrm{b}}(-\widehat{\boldsymbol{x}}_2) + \gamma_{\mathrm{b}}(-\widehat{\boldsymbol{x}}_3)\big) \approx I_{\mathrm{b}}\beta_{\mathrm{b}}(-\widehat{\boldsymbol{x}}_2), \tag{25d}$$

$$(L+M+S) \longrightarrow I_{\mathrm{w}}\widehat{\boldsymbol{x}}_3, \tag{25e}$$

$$-(L+M+S) \longrightarrow I_{\mathrm{s}}(-\widehat{\boldsymbol{x}}_3), \tag{25f}$$

where $\alpha_{\mathrm{k}}, \beta_{\mathrm{k}}, \gamma_{\mathrm{k}} \geq 0$, $\mathrm{k} = \mathrm{r, g, y, b}$, are constant parameters determined by the physiological or biophysical properties of the cells, whereas the coefficients $0 \leq I_{\mathrm{n}} \leq 1$, $\mathrm{n} = \mathrm{r, g, y, b, w, s}$, represent the intensity of the cells’ outputs. Notice that the mixed states in Eq. 25 are written in terms of Bloch vectors. Since these vectors must be contained within the Bloch ball, we have the constraint that $0 \leq {\alpha_{\mathrm{k}}}^2 + {\beta_{\mathrm{k}}}^2 + {\gamma_{\mathrm{k}}}^2 \leq 1$, $\mathrm{k} = \mathrm{r, g, y, b}$. The conspicuous difference between the bottom two equations and the upper four in Eq. 25 will be explained in Section 3.3. To sample Bloch space as fully as possible, the constant parameters in Eq. 25 should obey $\alpha_{\mathrm{r}} \gg \beta_{\mathrm{r}}, \gamma_{\mathrm{r}}$ in Eq. 25a, $\alpha_{\mathrm{g}} \gg \beta_{\mathrm{g}}, \gamma_{\mathrm{g}}$ in Eq. 25b, $\beta_{\mathrm{y}} \gg \alpha_{\mathrm{y}}, \gamma_{\mathrm{y}}$ in Eq. 25c, and $\beta_{\mathrm{b}} \gg \alpha_{\mathrm{b}}, \gamma_{\mathrm{b}}$ in Eq. 25d. This leads to the approximations shown on the right-hand side of Eqs. 25a–d. The decision of which of the Bloch vectors $\pm\hat{\boldsymbol{x}}_1$, $\pm\hat{\boldsymbol{x}}_2$ to take in each of the equations of Eq. 25 was based on the loci of unique hues in cone-excitation space (Webster et al., 2000). The decision of whether to take $+\hat{\boldsymbol{x}}_3$ or $-\hat{\boldsymbol{x}}_3$ in each of the Eqs. 25a–d was based on whether the spectral hue that the cell 'attempts' to encode is light or dark (spectral reds are darker than spectral greens, spectral yellows are lighter than blues (Gordon & Abramov, 1988)). Once the process of encoding is complete, the brain presumably combines the six ensembles of Eq. 25. It is the combined mixture that then undergoes QQST. Let us look at an example. Suppose that a region of the retina is illuminated with light whose spectral distribution is mostly concentrated around 574 nm, a wavelength that evokes a sensation of unique yellow (Webster et al., 2000). According to Eq. 25, the color-related physiological mechanisms would then create a qubit mixture whose resultant Bloch vector is in the vicinity of $+\hat{\boldsymbol{x}}_2$ (see Eq. 25c). When QQST is applied to this mixture, Eq. 24b shows that the phenomenal dual aspect will be of unique yellow.

Since the sampling of Bloch space specified in Eq. 25 relies on physiological mechanisms, it is not expected to be uniform, symmetric, or full; rather, we can expect this sampling to be non-uniform, asymmetric, and only partial. Consequently, our actual phenomenal color space, which is the dual aspect of the sampled part of Bloch space, will *not* be the spherical, uniform, and symmetric space of Fig. 3. Rather, it is expected to be irregular in shape, non-uniform, and asymmetric. The NCS color space, which, being a Hering-style color space, is a relative of the phenomenal color space of Fig. 3, confirms this prediction: it is grossly non-uniform, i.e., equal coordinate distances in it do not translate to equal perceptual distances (Kuheni, 2003, chapter 9; Kuehni, 2010; see Judd, 1968, for a discussion of uniformity in color spaces). Attempts to order our color percepts uniformly lead to color spaces with irregular shape, like the Munsell color space (Kuheni, 2003, chapter 2). Other asymmetries in our observed phenomenal color space are discussed in the next section.

3.3 Explaining the properties of color experience using H

The goal of this section is to show that H can explain various properties of color experience that are currently mysterious. To do this I will go through the questions posed in the *Introduction*, showing that using H we can give them elegant answers. For convenience, I repeat these questions here in bold.

Why are color percepts four-dimensional?

Color percepts have four dimensions because they are phenomenal dual aspects of the four parameters reconstructed by QQST, namely, the tetrad $(N, \boldsymbol{b})$ (or, put alternatively, $\langle\sigma_0\rangle_{\mathrm{u}}$ and $\langle\sigma_i\rangle$, $i = 1, 2, 3$).

What are the mechanisms that instantiate the three perceptual channels of opponent colors? (As we have seen, neurophysiology hasn't found these mechanisms.)

Ex hypothesi, the three perceptual channels of opponent colors (see right-hand side of Eqs. 23a–c) are phenomenal dual aspects of the three pairs of opponent processes on the left-hand side of Eqs. 23a–c.

Why do the outputs of the three color mechanisms fall into two phenomenally distinct groups (one achromatic, the other chromatic)? Or, looked at from a different perspective, why is it that the outputs of two of the three color mechanisms share a common phenomenal attribute (hue)?

Recall from Section 2.1 that when pure qubit states, which exist in $\mathbb{C}^2$, are mixed in an ensemble (or become entangled with other quantum systems), the resulting Bloch-space representation is in $\mathbb{R} \times \mathbb{C}$. (This 'demotion' is due to the loss of the global phase of qubit pure states; see details in Sections 2.1 and 2.2.) More specifically, as Eq. 17 shows, the Bloch vectors reconstructed by QQST are given by $\boldsymbol{b} = (\langle\sigma_3\rangle, \langle\sigma_1\rangle + i\langle\sigma_2\rangle)^{\mathrm{T}} \in \mathbb{R} \times \mathbb{C}$. Combining this expression for $\boldsymbol{b}$ with Eqs. 23a–c we see that the fact that the two chromatic channels have a shared phenomenal attribute (hue) that is different from the phenomenal attribute of the achromatic channel (lightness) has a mathematical correlate in Bloch space: the channels $\langle\sigma_1\rangle$ and $\langle\sigma_2\rangle$, which correspond to the chromatic channels in color space, belong to $\mathbb{C}$ in $\mathbb{R} \times \mathbb{C}$, whereas the channel $\langle\sigma_3\rangle$, which corresponds to the achromatic channel in color space, belongs to $\mathbb{R}$ in $\mathbb{R} \times \mathbb{C}$. To put things more succinctly, H suggests that (a) the mathematical attribute of belonging to the $\mathbb{C}$ component Bloch vectors gives rise to the phenomenal attribute of hue in color space; (b) the mathematical attribute of belonging to the $\mathbb{R}$ component of Bloch vectors gives rise to the phenomenal attribute of lightness in color space.

Why are there four unique hues? (Recall that neurophysiology hasn't found the neural correlates of these hues.)

In the previous answer it was suggested that the phenomenal attribute of hue is the dual aspect of the $\mathbb{C}$ component of Bloch vectors. We now notice from examining Figs. 2 and 3 that the four unique hues are phenomenal dual aspects of Bloch vectors that have a unique mathematical property: their $\mathbb{R}$ component is zero while their $\mathbb{C}$ component is *either exclusively real or exclusively imaginary*. Examples of this can be seen explicitly in Eqs. 24a–b for the case of the pure unique hues: they are the phenomenal dual aspects of the Bloch vectors $\pm\hat{\boldsymbol{x}}_1 = (0, \pm 1)^{\mathrm{T}}$ and $\pm\hat{\boldsymbol{x}}_2 = (0, \pm i)^{\mathrm{T}}$. Recall that the four unique hues are the unmixed examples of each of the four hue categories. We therefore see that according to H, mixed hues correspond to Bloch vectors whose $\mathbb{C}$ component mixes real and imaginary numbers; by contrast, Bloch vectors whose $\mathbb{C}$ component does not mix real and imaginary numbers give rise to unmixed hues, namely, to the unique hues.

Why is it that the gamut of all hues can be ordered in a closed continuum?

The answer to this age-old puzzle (Purves & Yegappan, 2017; Shepard, 1994) is clear from a comparison of Figs. 2 and 3: the hue circle is the phenomenal dual aspect of the complex unit circle in Bloch space. A comment is in place here, however. Recall from Section 3.2 that in the preparation of the ensemble that undergoes QQST the brain combines several mixed states together (see Eq. 25). As a result, the combined mixture cannot be in a pure state (unless the stimulus is of pure white or pure black because then Eqs. 25e–f do allow pure states, for $I_{\mathrm{w}} = 1$ or $I_{\mathrm{s}} = 1$). Consequently, the hue circle of pure hues that appears in Fig. 3 is unattainable by the brain. Attainable are only hue circles whose hues are not 100% pure. (Note that this is essentially due to the same reasons discussed in the *Introduction* of why three independent opponent-processes mechanisms lead to a hue square rather than a hue circle.) This is indeed what is observed: even the purest hues, which are evoked by spectral colors, do not exhibit 100% purity (Gordon & Abramov, 1988). This inability of the brain to fully sample Bloch space relates to the discussion at the end of Section 3.2 as to the implications of the non-uniform and only partial sampling of Bloch space by the brain.

Why is it that white and black, i.e., the two achromatic opponent colors, can perceptually coexist in one color, but the two elementary colors of each of the chromatic opponent pairs are mutually exclusive?

If we substitute Eq. 21 into the left-hand side of Eq. 22, we obtain the same correspondences as in Eqs. 23a–c but formulated in a way that will give us more insight:

$$\langle\sigma_1\rangle = \langle|+\hat{\boldsymbol{x}}_1\rangle\langle+\hat{\boldsymbol{x}}_1|\rangle - (1 - \langle|+\hat{\boldsymbol{x}}_1\rangle\langle+\hat{\boldsymbol{x}}_1|\rangle) \leftrightarrow R - G, \tag{26a}$$

$$\langle\sigma_2\rangle = (1 - \langle|-\hat{\boldsymbol{x}}_2\rangle\langle-\hat{\boldsymbol{x}}_2|\rangle) - \langle|-\hat{\boldsymbol{x}}_2\rangle\langle-\hat{\boldsymbol{x}}_2|\rangle \leftrightarrow Y - B, \tag{26b}$$

$$\langle\sigma_3\rangle = \langle|+\hat{\boldsymbol{x}}_3\rangle\langle+\hat{\boldsymbol{x}}_3|\rangle - \langle|-\hat{\boldsymbol{x}}_3\rangle\langle-\hat{\boldsymbol{x}}_3|\rangle \leftrightarrow W - S. \tag{26c}$$

Separating each of the correspondences in Eq. 26 into its constituents we find

$$\langle|+\hat{\boldsymbol{x}}_1\rangle\langle+\hat{\boldsymbol{x}}_1|\rangle \leftrightarrow R, \tag{27a}$$

$$1 - \langle|+\hat{\boldsymbol{x}}_1\rangle\langle+\hat{\boldsymbol{x}}_1|\rangle \leftrightarrow G = 1 - R, \tag{27b}$$

$$\langle|-\hat{\boldsymbol{x}}_2\rangle\langle-\hat{\boldsymbol{x}}_2|\rangle \leftrightarrow B, \tag{27c}$$

$$1 - \langle|-\hat{\boldsymbol{x}}_2\rangle\langle-\hat{\boldsymbol{x}}_2|\rangle \leftrightarrow Y = 1 - B, \tag{27d}$$

$$\langle|+\hat{\boldsymbol{x}}_3\rangle\langle+\hat{\boldsymbol{x}}_3|\rangle \leftrightarrow W, \tag{27e}$$

$$\langle|-\hat{\boldsymbol{x}}_3\rangle\langle-\hat{\boldsymbol{x}}_3|\rangle \leftrightarrow S. \tag{27f}$$

Notice that $G = 1 - R$ and $Y = 1 - B$. That is, G and Y *do not exist as independent processes*.[7] To directly see the implications of this realization, we substitute Eq. 27 back into Eq. 26, slightly reorganize terms, and obtain

$$\langle\sigma_1\rangle = 2\langle|+\hat{\boldsymbol{x}}_1\rangle\langle+\hat{\boldsymbol{x}}_1|\rangle - 1 \leftrightarrow 2R - 1, \tag{28a}$$

$$\langle\sigma_2\rangle = 1 - 2\langle|-\hat{\boldsymbol{x}}_2\rangle\langle-\hat{\boldsymbol{x}}_2|\rangle \leftrightarrow 1 - 2B, \tag{28b}$$

$$\langle\sigma_3\rangle = \langle|+\hat{\boldsymbol{x}}_3\rangle\langle+\hat{\boldsymbol{x}}_3|\rangle - \langle|-\hat{\boldsymbol{x}}_3\rangle\langle-\hat{\boldsymbol{x}}_3|\rangle \leftrightarrow W - S. \tag{28c}$$

Equation 28 explains why the two elementary colors in the achromatic opponent pair, i.e., white and black, can be simultaneously perceived in one color, whereas the two elementary colors of each of the chromatic opponent pairs are mutually exclusive. Let us start with Eq. 28c. Since both the expectation values $\langle|+\hat{\boldsymbol{x}}_3\rangle\langle+\hat{\boldsymbol{x}}_3|\rangle$ and $\langle|-\hat{\boldsymbol{x}}_3\rangle\langle-\hat{\boldsymbol{x}}_3|\rangle$

---

[7] Of course, we could have chosen R and B as the dependent processes. Here they are the independent processes only because in Eq. 21 we arbitrarily chose to measure the probability of the state $|+\hat{\boldsymbol{x}}_1\rangle$ from the pair $|\pm\hat{\boldsymbol{x}}_1\rangle$ and the probability of the state $|-\hat{\boldsymbol{x}}_2\rangle$ from the pair $|\pm\hat{\boldsymbol{x}}_2\rangle$.

are measured during QQST, both their corresponding processes in color space, i.e., W and S, respectively, *exist as independent processes*. As a result, we have conscious access to both the white and black contents of a color percept. By contrast, Eqs. 27a–b argue that the outputs of the two chromatic channels *do not arise from a pair of opponent processes*. That is, in stark contrast to the achromatic channel, in the chromatic channels there are no two separate and independent processes. Rather, each of these channels exists as a one-dimensional continuum that stretches from -1 to 1. Thus, we never perceive red and green simultaneously because there are no separate red and green processes; there is only one process whose extremum values are pure unique red and pure unique green. The same, *mutatis mutandis*, applies to yellow and blue.

Why do colors additively mix according to the center of gravity principle (Eq. 2)?

This is because Eq. 2 for colors is the phenomenal dual of Eq. 15 for Bloch vectors.

How is it that the phenomenal color space of dichromats is three-dimensional? Why, then, is the phenomenal color space of monochromats only one-dimensional and restricted to lightness?

Let us take of example a dichromat who is a protanope (missing the L-cone). Presumably, the $(L - M)$- and $(M - L)$-cells in this person are not functional. However, the $\big((L+M)-S\big)$- and $\big(S-(L+M)\big)$-cells do survive, albeit as $(M-S)$- and $(S-M)$-cells. Now, according to Eqs. 25c–d, these cells will encode Bloch vectors that have some small components in the $\pm\hat{\boldsymbol{x}}_1$ directions. Consequently, when QQST applies measurements along the $\pm\hat{\boldsymbol{x}}_1$ directions (Eq. 23a), the result of these measurements will not be zero. We conclude that residual red or green perceptions will be evoked in such a person. Since the components along the $\pm\hat{\boldsymbol{x}}_1$ directions are small, the size of the stimulus, its intensity, and its purity must be high, as indeed observations show (Broackes, 2010). The explanations for the other types of dichromats are analogous.

For monochromats, the situation is different. Since a monochromat has only a single type of cone functional, the physiological channels $(L-M)$, $(M-L)$, $\big((L+M)-S\big)$, and $\big(S-(L+M)\big)$ are all inactive. The only surviving physiological channels are $(L+M+S)$ and $-(L+M+S)$, but they collapse to $L/M/S$ and $-L/-M/-S$, depending on which cone is functional. Since the data shows that the phenomenal color space of monochromats is one-dimensional and is restricted to lightness (Nordby, 1990; Sharpe et al., 1999), we must conclude that the mixture encoding performed by the physiological channels $(L+M+S)$ and $-(L+M+S)$ has only $\pm\hat{\boldsymbol{x}}_3$ components without any $\pm\hat{\boldsymbol{x}}_1$ or $\pm\hat{\boldsymbol{x}}_2$ components. Otherwise, QQST along the $\pm\hat{\boldsymbol{x}}_1$, $\pm\hat{\boldsymbol{x}}_2$ directions in Bloch space (Eqs. 23a–b) would not yield zero and the monochromat would have residual hue perception. Therefore, Eqs. 25e–f show an exact encoding along the $\pm\hat{\boldsymbol{x}}_3$ directions. Now, this hypothesized ability of the physiological channels $(L+M+S)$ and

$-(L + M + S)$ to prepare a mixed state *exactly* along the $\pm\hat{\boldsymbol{x}}_3$ components in Bloch space is suspicious. How can such precision be accomplished? The only way this can be accomplished is if the encoding along the $\pm\hat{\boldsymbol{x}}_3$ components and the measurement along these directions *use the same physical process*.

As an aside, notice that the meaning of Eqs. 25e–f is the brain is able to generate pure quantum states in the case of pure white and pure black stimuli. In other words, when a person views a strong white stimulus, H predicts that somewhere in the brain there should be an ensemble of qubits in a pure state. This prediction could perhaps serve in the future to locate the qubit system that presumably gives rise to our color sensations.

What is the nature of the relationship between lightness and brightness? Do they indeed share a single dimension?

Equation 23d allows us to multiply the left- and right-hand sides of Eq. 23c by N and Q, respectively. Using Eq. 19 and Eqs. 26e–f we then arrive at the following correspondence

$$\langle|+\hat{\boldsymbol{x}}_3\rangle\langle+\hat{\boldsymbol{x}}_3|\rangle_{\mathrm{u}} \leftrightarrow W_{\mathrm{u}}, \tag{29a}$$

$$\langle|-\hat{\boldsymbol{x}}_3\rangle\langle-\hat{\boldsymbol{x}}_3|\rangle_{\mathrm{u}} \leftrightarrow S_{\mathrm{u}}, \tag{29b}$$

where $W_{\mathrm{u}} = Q \cdot W$ and $S_{\mathrm{u}} = Q \cdot S$ are the unnormalized versions of the processes W and S. (Note that because in reality W_{u} and S_{u} precede W and S, these relationships should actually be written as $W = W_{\mathrm{u}}/Q$ and $S = S_{\mathrm{u}}/Q$.) From Eq. 24d and Eq. 29, we see that the color-space equivalent of Eq. 20 is

$$W_{\mathrm{u}} + S_{\mathrm{u}} = Q. \tag{30}$$

Equation 30 answers both questions above. First, it clarifies the relationship between lightness and brightness: the basic constituents of both lightness and brightness are whiteness and blackness. More specifically, lightness arises from the difference of the normalized values of whiteness and blackness (Eq. 28c); brightness arises from the sum of the unnormalized values of whiteness and blackness (Eq. 30). Second, Eq. 30 makes it clear that in general lightness and brightness do *not* share a single dimension, as has been claimed (Gilchrist, 2006, chapter 9). Rather, lightness and brightness are distinct mathematically (compare Eq. 28c and Eq. 30) and therefore distinct phenomenally. However, Eq. 30 also explains why an identity between brightness and whiteness occurs for unrelated achromatic colors (Shevell, 2003) and for related achromatic colors at high levels of luminance (Gilchrist, 2006, chapter 9). In both these cases we can take the value of S_{u} in Eq. 30 to be zero. Consequently, this equation simplifies to

$$W_{\mathrm{u}} = Q, \tag{31}$$

which is exactly the observed phenomenon.

Notice that together Eq. 28c and Eq. 30 make a testable prediction: for a constant level of whiteness in a color, increasing the blackness level should decrease the color's lightness and increase its brightness (and vice versa). In other words, for a constant level of whiteness, brightness should increase as lightness decreases. This prediction is beautifully confirmed in spectral colors. Violet (400 nm) is both the brightest and the darkest spectral color, while yellow (580 nm) is both the least bright and the lightest spectral color (Shevell, 2003). Similarly, spectral colors above 610 nm (which appear yellowish-red or red) are both brighter and darker than spectral colors in the range 480–510 nm (which appear bluish-green or green) (*ibid*.).[8]

4. Discussion

The properties of our color experience have been studied for centuries. Although vast amounts of perceptual, psychophysical, and neurophysiological data on color experience have been accumulated, explanations for its phenomenal properties are still lacking. It was shown here that some of these phenomenal properties can be explained if it is hypothesized that our color percepts are the phenomenal dual aspects of qubit mixed states reconstructed through quantum state tomography.[9] (For conciseness, this hypothesis was denoted H.) As Section 3.3 showed in detail, an intriguing feature of the proposed dual-aspect theory is that it suggests that the mathematical properties of

[8] These comparisons of brightness and lightness of spectral colors were all performed at *equal luminance levels*. I am assuming here that equal luminance levels also mean equal whiteness levels. To see why, note that the luminance level at a particular wavelength results from the product of the light energy at the wavelength and the luminous efficiency of the wavelength, denoted V_λ (Lennie et al., 1993). Following Hurvich and Jameson (1957), I am taking the *whiteness spectral sensitivity function* to be identical to the luminous efficiency function. This assumption is supported by the fact that—as was predicted by Hurvich and Jameson—the luminous efficiency for (induced) blackness is exactly the inverse of the luminous efficiency function (Cicerone et al., 1986; Werner et al., 1984). Given that the whiteness spectral sensitivity function equals the luminous efficiency function, equal luminance levels mean equal whiteness levels, as required.

[9] Remarkably, the nomenclatures used in color science and in quantum mechanics are virtually identical: both fields use a terminology of pure states and mixtures. I do not know whether the quantum mechanical nomenclature, which evolved somewhat later than the one of color science, was affected by the latter.

qubit mixed states are ‘translated’ in a law-like manner to phenomenal properties of color percepts. This ‘translation’ does not—and cannot—explain why color has the specific intrinsic *qualities* that it has (the redness of red, the greenness of green, etc.). What it does explain, however, is the *properties* of these qualities. For example, one of the great successes of H is that it explains why white and black, i.e., the two achromatic opponent colors, can perceptually coexist in one color, whereas the two elementary colors of each of the chromatic opponent pairs (red–green and yellow–blue) are mutually exclusive. Another important example is the ability of H to solve the riddle of why the gamut of all hues can be ordered in a *closed* continuum. If, as H argues, phenomenal properties are dual aspects of mathematical properties of a physical system, then it must be the case that mathematical properties of physical systems *really* exist (of course, this assumes that our consciousness really exists, something that I take to have been proven by Descartes). Such a possibility dovetails nicely with an ontological world view advocated by Tegmark (2008) and Carroll (2022) (also see Woit, 2015) wherein the physical world around us is not merely *described* by mathematical objects and equations, but in fact *is* those objects and equations. A glaring lacuna in a such an ontology, however, is the absence of phenomenal experience. If we generalize H to other types of phenomenal experience, it could fill this lacuna. On this generalization, *all* types of phenomenal experience (color, taste, odor, sound, etc.) are dual aspects of quantum states reconstructed through quantum state tomography. Quantum systems that are more complex than a qubit, which is the simplest quantum system, are expected to give rise to types of phenomenal experience than are more complex than color (notice, then, that on this hypothesis, color is the simplest type of phenomenal experience).

Naturally, an unorthodox hypothesis such as H raises a host of issues and questions. What is the identity of the hypothesized qubit mixture? How exactly does the brain create and 'encode' this mixture (see Section 3.1)? What is the system performing the QQST? And a myriad of other hard questions. Since we don't have answers to these questions, it would be best if we could simply test H directly. There might just be a way to do that. In a recent work, Forder et al. (2017) have found a neural signature of the unique hues: event-related potentials (ERPs) evoked by unique hues peaked significantly earlier than ERPs evoked by non-unique hues. A slight expansion of Forder et al.'s experiments may be used to test H. Since QQST is a serial process (see details in Section 2.4), information regarding the brightness, lightness (i.e., white–black), red–green, and yellow–blue components of a color is collected *successively*. Specifically, the quantum measurements that give rise to brightness and lightness are most likely performed before the measurements that give rise to hue. Therefore*, assuming that the ERPs recorded by Forder et al. are echoes of the presumed QQST process*, we can expect the ERPs of achromatic colors to peak before the ERPs of the unique hues.

5. References

Aerts, D. & Sassoli de Bianchi, M. (2017). Do spins have directions? *Soft Computing*, *21*(6), 1483–1504.

Altepeter, J. B., James, D. F. V., & Kwiat, P. G. (2004). Qubit quantum state tomography. In Paris, M. G. A. & Řeháček, J. (Eds.), *Quantum State Estimation*. Berlin, Heidelberg: Springer.

Bertlmann, R. A. & Krammer, P. (2008). Bloch vectors for qudits. *Journal of Physics A: Mathematical and Theoretical*, *41*(23), p. 235303.

Blum, K. (1981). *Density Matrix Theory and Applications*. New York and London: Plenum Press.

Bohon, K. S., Hermann, K. L., Hansen, T., & Conway, B. R. (2016). Representation of perceptual color space in macaque posterior inferior temporal cortex (the V4 complex). *eNeuro*, *3*(4), 1–28.

Boynton, R. M. (1979). *Human Color Vision*. New York: Holt, Rinehart and Winston.

Broackes, J. (2010). What do the color-blind see? In Cohen, J. & Matthen, M. (Eds.), *Color Ontology and Color Science*. Cambridge, Massachusetts: MIT Press.

Broackes, J. (2011). Where do the unique hues come from? *Review of Philosophy and Psychology*, *2*(4), 601–628.

Byrne, A. & Hilbert, D. R. (2010). How do things look to the color-blind? In Cohen, J. & Matthen, M. (Eds.), *Color Ontology and Color Science*. Cambridge, Massachusetts: MIT Press.

Carroll, S. M. (2022). Reality as a vector in Hilbert space. In Allori, V. (Ed.), *Quantum Mechanics and Fundamentality: Naturalizing Quantum Theory between Scientific Realism and Ontological Indeterminacy*. Springer.

Chalmers, D. J. (1996). *The Conscious Mind: In Search of a Fundamental Theory*. New York: Oxford University Press.

Cicerone, C. M., Volbrecht, V. J., Donnelly, S. K., & Werner, J. S. (1986). Perception of blackness. *Journal of the Optical Society of America A*, *3*(4), 432–436.

Cortês, M., Smolin, L., & Verde., C. (2021). Physics, time, and qualia. *Journal of Consciousness Studies*, *28*(9–10), 36–51.

Derrington, A. M., Krauskopf, J., & Lennie, P. (1984). Chromatic mechanisms in lateral geniculate nucleus of macaque. *The Journal of Physiology*, *357*(1), 241–265.

De Monasterio, F. M., Gouras, P., & Tolhurst, D. J. (1975). Trichromatic colour opponency in ganglion cells of the rhesus monkey retina. *The Journal of Physiology*, *251*(1), 197–216.

De Valois, R. L., Abramov, I., & Mead, W. R. (1967). Single cell analysis of wavelength discrimination at the lateral geniculate nucleus in the macaque. *Journal of Neurophysiology*, *30*(3), 415–433.

Forder, L., Bosten, J., He, X., & Franklin, A. (2017). A neural signature of the unique hues. *Scientific Reports*, *7*(1), 1–8.

Gilchrist, A. (2006). *Seeing Black and White*. Oxford University Press.

Gilchrist, A. L. (2007). Lightness and brightness. *Current Biology*, *17*(8), R267–R269.

Gouras, P. (1968). Identification of cone mechanisms in monkey ganglion cells. *The Journal of Physiology*, *199*(3), 533–547.

Gordon, J. & Abramov, I. (1988). Scaling procedures for specifying color appearance. *Color Research & Application*, *13*(3), 146–152.

Hård, A., Sivik, L. & Tonnquist, G. (1996). NCS, natural color system—from concept to research and applications. Part I. *Color Research & Application*, *21*(3), 180–205.

Hurvich, L. M. (1981). *Color Vision*. Sunderland, Mass.: Sinauer Associates.

Hurvich, L. M. & Jameson, D. (1957). An opponent-process theory of color vision. *Psychological Review*, *64*(6), 384–404.

Judd D. B. (1968). Ideal color space. II. The super-importance of hue differences and its bearing on the geometry of color space. *Palette*, 30, 21–28.

Kuheni, R. G. (2010). Color spaces and color order systems: A primer. In Cohen, J. & Matthen, M. (Eds.), *Color Ontology and Color Science*. Cambridge, Massachusetts: MIT Press.

Kuheni, R. G. (2003). *Color Space and its Divisions*. Hoboken, New Jersey: John Wiley & Sons.

Lennie, P., Krauskopf, J., & Sclar, G. (1990). Chromatic mechanisms in striate cortex of macaque. *Journal of Neuroscience*, *10*(2), 649–669.

Lennie, P., Pokorny, J., and Smith, V. C. (1993). Luminance. *Journal of the Optical Society of America A*, *10*(6), 1283–1293.

Lockwood, M. (1989). *Mind, Brain, and the Quantum: The Compound 'I'*. New York, NY: Blackwell.

Mollon, J. (2006). Monge: The Verriest lecture, Lyon, July 2005. *Visual Neuroscience*, *23*(3–4), 297–309.

Mollon, J. D. (2009). A neural basis for unique hues? *Current Biology*, *19*(11), R441–R442.

Mollon, J. D. (1982). A taxonomy of tritanopias. *Documenta Ophthalmologica Proceedings Series*, *33*, 87–101.

Nordby, K. (1990). Vision in a complete achromat: a personal account. In Hess, R. F., Sharpe, L., & Nordby, K. (Eds.), *Night Vision: Basic Clinical and Applied Aspects*. Cambridge: Cambridge University Press.

Palmer, S. E. (1999). *Vision Science: Photons to Phenomenology*. MIT press.

Purves, D., Lotto, B., & Polger, T. (2000). Color vision and the four-color-map problem. *Journal of Cognitive Neuroscience*, *12*(2), 233–237.

Purves, D. & Yegappan, C. (2017). The demands of geometry on color vision. *Vision*, *1*(1), p. 9.

Sharpe, L. T., Stockman, A., Jägle, H., & Nathans, J. (1999). Opsin genes, cone photopigments, color vision, and color blindness. In Gegenfurtner, K. R. & Sharpe, L. T. (Eds.), *Color Vision: From Genes to Perception*. Cambridge: Cambridge University Press.

Shepard, R. N. (1994). Perceptual-cognitive universals as reflections of the world. *Psychonomic Bulletin & Review*, *1*, 2–28.

Shepard, R. N. (1992). The perceptual organization of colors: An adaptation to regularities of the terrestrial world. In Barkow, J. H., Cosmides, L., & Tooby, J. (Eds.), *The Adapted Mind: Evolutionary Psychology and the Generation of Culture*. Oxford: Oxford University Press.

Shevell, S. K. (2003). Color appearance. In Shevell, S. K. (Ed.), *The Science of Color*. Elsevier.

Stubenberg, L. (2018). Neutral monism. In Zalta, E. N. (Ed.), *The Stanford Encyclopedia of Philosophy*. URL = https://plato.stanford.edu/archives/fall2018/entries/neutral-monism/

Tegmark, M. (2008). The mathematical universe. *Foundations of Physics*, *38*(2), 101–150.

Valberg, A. (2001). Unique hues: an old problem for a new generation. *Vision Research*, *41*(13), 1645–1657.

Webster, M. A., Miyahara, E., Malkoc, G., & Raker, V. E. (2000). Variations in normal color vision. II. Unique hues. *Journal of the Optical Society of America A*, *17*(9), 1545–1555.

Werner, J. S., Cicerone, C. M., Kliegl, R., & DellaRosa, D. (1984). Spectral efficiency of blackness induction. *Journal of the Optical Society of America A*, *1*(9), 981–986.

Woit, P. (2015). Towards a grand unified theory of mathematics and physics. *arXiv preprint arXiv:1506.07576*.